materials

MDPI

Communication

A Century of General Lichtenecker Equation: Between Stringency and Empiricism, Accuracy and Approximability

Anatoliy V. Goncharenko [1,2,*] and Vyacheslav M. Silkin [2,3,4]

[1] V.E. Lashkaryov Institute of Semiconductor Physics, 41 Nauky Ave., 03028 Kyiv, Ukraine
[2] Donostia International Physics Center (DIPC), 20018 San Sebastian, Basque Country, Spain
[3] Departamento de Polímeros y Materiales Avanzados: Física, Química y Tecnología, Facultad de Ciencias Químicas, Universidad del País Vasco UPV/EHU, 20080 San Sebastian, Basque Country, Spain
[4] IKERBASQUE, Basque Foundation for Science, 48013 Bilbao, Basque Country, Spain
* Correspondence: avg@isp.kiev.ua

Abstract

The general Lichtenecker equation, with exponent values in the range $-1 \leq k \leq 1$, is widely used to describe and predict the effective macroscopic electrical, magnetic, thermal and optical properties of various heterogeneous media. Although it sometimes fits experimental data well, in most cases, however, it is physically incorrect and its predictive ability is often overestimated. Using a rigorous spectral representation, we show that for isotropic composites, except for the trivial one-dimensional case, only two specific forms of this equation, the logarithmic ($k = 0$) and Landau-Lifshitz-Looyenga ($k = 1/3$) mixing laws, are dimensionally consistent, corresponding to spatial dimensions $d = 2$ and $d = 3$, respectively. Furthermore, the requirement of phase-interchange symmetry severely restricts the applicability of the Lichtenecker equation, rendering it unsuitable for most real composite systems.

Keywords: effective medium; homogenization; Lichtenecker equation; Archie's law; spectral representation

check for updates

Academic Editor: Zhonghua Yao

Received: 17 November 2025
Revised: 3 December 2025
Accepted: 8 December 2025
Published: 11 December 2025

Citation: Goncharenko, A.V.; Silkin, V.M. A Century of General Lichtenecker Equation: Between Stringency and Empiricism, Accuracy and Approximability. *Materials* **2025**, *18*, 5562. https://doi.org/10.3390/ma18245562

Copyright: © 2025 by the authors. Licensee MDPI, Basel, Switzerland. This article is an open access article distributed under the terms and conditions of the Creative Commons Attribution (CC BY) license (https://creativecommons.org/licenses/by/4.0/).

1. Introduction

Many researchers and engineers face the problem of expressing the effective macroscopic response (such as permittivity, conductivity, diffusivity, etc.) of various heterogeneous media, including dielectric composites, porous materials, disordered systems. Perhaps the most popular approach is based on phenomenological effective medium (homogenization) theories. Three of them, associated with the names of Maxwell Garnett, Bruggeman and Lichtenecker, are especially frequently used.

In 2026, it is a century as Karl Lichtenecker first put forward his empirical mixing rules [1]. The original equation for the effective permittivity ϵ_{eff} in its general form was

$$\epsilon_{eff}^k = f_1\epsilon_1^k + f_2\epsilon_2^k, \tag{1}$$

where f_1 and f_2 are the volume fractions of the phases 1 and 2, respectively, ϵ_1 and ϵ_2 are their permittivities, and k is a phenomenoligical parameter. The value of k in Equation (1) is constrained by the Wiener bounds, i.e., $-1 \leq k \leq 1$, and is often considered as a fitting parameter.

In his earlier paper [2], Lichtenecker also proposed an equation of the form

$$\log(\epsilon_{eff}) = f_1 \log(\epsilon_1) + f_2 \log(\epsilon_2), \tag{2}$$

which can in fact be considered as a particular case of Equation (1) in the limit $k \to 0$. The main assumption made in deriving Equation (2) is a random distribution of particle shapes and orientations for each phase such that the charge density within any phase can be replaced by the mean charge density of the mixture. This allows one to replace the charge fractions with their volume fractions [3].

In the literature, Equation (2) is also frequently called as Lichtenecker equation. To avoid confusion, in the following we refer to Equation (1) with arbitrary k as the general Lichtenecker equation (LE), while Equation (2) is referred to as the logarithmic Lichtenecker equation (LLE). As can be seen, Equation (1) represents the weighted arithmetic and harmonic means at $k = 1$ and $k = -1$, respectively, while Equation (2) represents the weighted geometric mean.

The LE has been widely used or tested to describe and predict effective permittivity, permeability, electric, thermal and hydraulic conductivity of diverse natural and artificial mixtures—liquids, solids, powders, metal composites, etc. Particular examples include the permittivity of emulsions [4,5], soils [6], multiwalled carbon nanotube/polymer nanocomposites [7], nanoparticle doped elastomeric polymers [8], fabric aggregates [9], metal nanopowders [10,11], concrete [12], Lunar and asteroid regolith [13], barium titanate based composites [14], alcali brick composites [15], piezoelectric ceramics [16]; the electric conductivity of shaly sandstones [17] and sedimentary rocks [18]; the thermal conductivity of mineral wools [19] and sedimentary rocks [20]; the magnetic permeability of ferrite/polymer composites [21,22].

While the values of the parameter k may lie within the range from -1 to 1, both edges of this interval are associated with a strong anisotropy [16,23,24]. In this study we focus mainly on isotropic systems. Our aim is to clarify the physical premises underlying the LE and to establish a set of fundamental limitations that govern its validity. While this equation is widely used, it appears to be overstated and, in fact, its area of applicability is rather limited. In the following we show this using simple physical arguments involving the formalism of spectral representation.

2. Geometry and Percolation

Taking look at Equation (1), several immediate conclusions can be made. First, it is a symmetric approximation in which both phases are treated equally. This means that the matrix (host) and inclusions are indistinguishable: every phase can be regarded as the host or as the inclusion, and the corresponding composite media should possess phase-inversion symmetry [25]. Thus, the microgeometry of each phase is completely identical to that of the other. The geometry must be such that both phases interpenetrate in a comparable manner (neither is clearly an inclusion within the other), as in bicontinuous or lamellar structures, symmetric random blends, etc. If we swap phases 1 and 2, the geometry remains the same and the effective property relation remains unchanged, that reflects its invariance.

Another important point is that, as the LE assumes, for the corresponding microgeometry both phases must topologically percolate at any volume fractions f_i, if only $k \geq 0$. Indeed, as is easy to see that, in terms of conductivity, $\sigma_{eff} \to \infty$ if any $\sigma_i \to \infty$.

Most real composite systems, of course, do not satisfy the above conditions of symmetry and percolation. Moreover, as will be shown below, even if both above conditions are met, it does not necessarily follow that Equation (1) holds.

3. Spectral Density Function Analysis

To take a step forward, let us now consider the LE in terms of the spectral representation. It should be noted that this representation is conceptually analogous to the rigorous Green´s function formalism, which is known to be the backbone of many approaches

in condensed matter physics. Within the framework of the spectral representation, the effective permittivity $\tilde{\epsilon}$ can be expressed as [26–29]

$$\tilde{\epsilon}_{eff}/\epsilon_1 \equiv \tilde{\epsilon} = 1 + f_2\left(\frac{C_2}{s_2} + \int_0^1 \frac{g_2(x)dx}{s_2 + x}\right), \tag{3}$$

where $s_2 = (\epsilon_2/\epsilon_1 - 1)^{-1}$ and x plays the role of a spectral variable linked to depolarization factors. The function $g_2(x)$ contains the necessary information about the microgeometry of the composite and is referred to as the spectral density function (SDF) [28,30–32]. The SDF is similar to the density of states (DOS) in electronic structure theory which, in turn, is known to have a profound significance in disordered systems, where the Bloch theory becomes inapplicable. While the DOS gives us the distribution of electronic states over energy, independent of the specific interaction strength, the SDF specifies how geometrical modes, associated with polarization resonances, are distributed, independent of the material constants of constituents. Thus, the SDF highlights how disorder and geometry manifest themselves as distributions of modes, rather than through deterministic parameters.

Any effective material property, such as permittivity, permeability, electric, thermal or hydraulic conductivity, or a diffusion coefficient can be expressed as a function of a contrast parameter h, which can be defined as $h = \epsilon_2/\epsilon_1$ or $h = \sigma_2/\sigma_1$ in terms of the permittivity or electric conductivity, respectively. For electromagnetic quantities (permittivity, permeability and electrical conductivity), the material parameters are typically strongly frequency dependent. As a result, the parameter $h(\omega)$ (and correspondingly $s_2 = (h-1)^{-1}$) can vary over several orders of magnitudes across a broad frequency range. This, in general, makes it possible to recover the SDF from experimental data, provided that measurements of the effective property are available over a sufficiently wide and densely sampled range of contrast parameter values, usually achieved by a wide frequency sweep.

Conversely, thermal conductivity, hydraulic conductivity and diffusion coefficient generally do not exhibit significant frequency dependence. Instead, these quantities may vary with temperature. The corresponding effective properties can be regarded as temperature-dependent, so that the contrast parameter can be tuned through temperature variation. A similar approach may be also applicable to magnetic properties in materials, where the permeability changes substantially with temperature, particularly near magnetic phase transition.

The SDF in Equation (3) is normalized to unity:

$$\int_0^1 g_2(x)dx = 1 - C_2. \tag{4}$$

In addition, for a system possessing a cubic or isotropic rotational symmetry, its first moment is known to satisfy the sum rule

$$\int_0^1 x g_2(x)dx = \frac{f_1}{d}, \tag{5}$$

where d is the spatial dimensionality of the system.

The spectral density function for the classical Maxwell Garnett and Bruggeman theories is well known [33]. For the LE (1), this function was derived earlier in [34]. Although these result are correct, the SDF can be represented in a very neat compact form using complex notation. As can be checked, if $k \neq 0$, it is simply

$$g_2(x) = \frac{1}{\pi f}\Im[1 - f + ft^k \exp(ik\pi)]^{1/k}, \tag{6}$$

where $t = 1/x - 1$. For some particular cases, SDF takes especially simple forms. At $k = 1/2$ (the so-called CRIM— complex-refractive-index-model) it is [26]

$$g_2(x) = \frac{2}{\pi}(1-f)(\frac{1}{x}-1)^{1/2}. \quad (7)$$

At $k = 1/3$, for the so-called Landau-Lifshitz-Looyenga (LLL) equation [35,36]

$$g_2(x) = \frac{3^{3/2}}{2\pi}(1-f)(\frac{1}{x}-1)^{1/3}. \quad (8)$$

At $k = 0$, for the LLE [34],

$$g_2(x) = \frac{\sin(\pi f)}{\pi f}(\frac{1}{x}-1)^{f}. \quad (9)$$

Consider next the first moment of the SDF. Substituting Equation (6) into Equation (5) allows one to find a relationship between the parameters k and d. After bulky calculations, the final result is unexpectedly simple:

$$d = 2\frac{1+\frac{1}{6}k}{1-\frac{5}{6}k-\frac{1}{6}k^2}. \quad (10)$$

The dependence $d(k)$ is shown in Figure 1. In particular, we have $d = 2$ at $k = 0$, $d = 3$ at $k = 1/3$, and $d = 4$ at $k = 1/2$. As $k \to -1$, $d \to 1$. Consider then the relationship between k and d in more details.

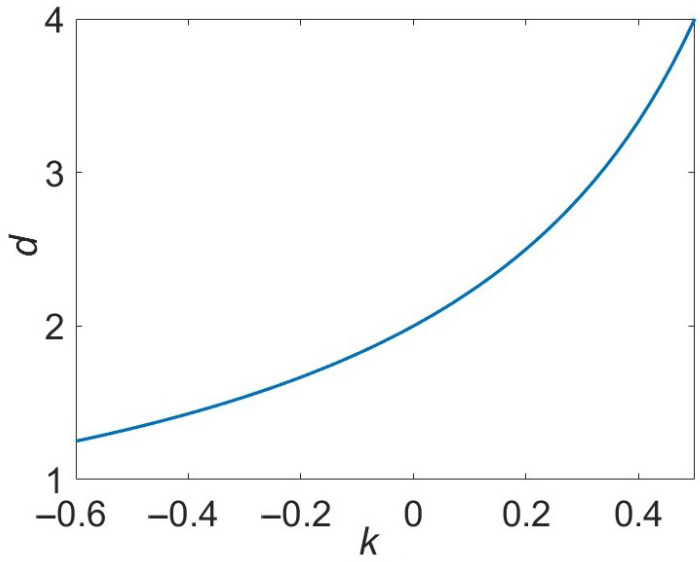


Figure 1. The dependence of $d(k)$ in accordance with Equation (10).

4. The Parameter k and the Issue of Dimensionality

In the case of $k = -1$, $d = 1$ and the corresponding microgeometry can be imagined as a layered periodic system in which the displacement field, magnetic induction, electric or thermal currents, or heat or mass flux are directed normal to the layers. We note that this direction is the only one that is defined in one dimension. As the ratio of the 1D lattice period to a macroscopic length scale (such as the wavelength of light, characteristic scales of potential or temperature variation, or diffusion length) tends to zero, LE is known to be exact.

The case of $k = 0$ yields $d = 2$ and results in the LLE, Equation (2), which is particularly frequently used to describe various effective physical characteristics of composite media.

The main results for 2D systems have been obtained with the use of the Keller-Dykhne duality relation [37,38].

It is well-known that in 2D systems with $f_1 = f_2 = 1/2$, which possess phase-inversion symmetry, the equation

$$\tilde{\epsilon}_{eff} = \sqrt{\epsilon_1 \epsilon_2} \tag{11}$$

holds, independently of the specific microgeometry. It is easy to see that Equation (11) follows from Equation (2) when $f_1 = f_2 = 1/2$. In addition, using Equation (11) one can verify that Equation (2) coincides with the 2D symmetric Bruggeman equation.

What happens if $f_1 \neq f_2$? Significant progress in this direction was achieved by Machavariani and Fel [39,40]. They began with the microgeometry of a 2D regular infinite checkerboard and assumed that each square on this checkerboard is itself non-uniform, being composed of smaller (finite) checkerboards. By repeating this recursive procedure indefinitely, Equation (2) can be recovered as the result of an interpolation. However, if the recursion is terminated at a finite stage, Equation (2) becomes approximate. It is important that due to the Keller-Dykhne duality, not only square lattices but also trianglular ones and random spot distributions lead to similar conclusions.

Naturally, the key point is the accuracy of this approximation. To quantify it, Machavariani performed numerical calculations of the effective conductivity for various regular 2D structures [40]. The obtained results show that the discrepancy between the numerically obtained effective conductivity and Equation (2) depends markedly on the phase contrast σ_1/σ_2, with the deviations remaining small for a low contrast, specifically for $0.2 \leq \sigma_1/\sigma_2 \leq 5$. These findings were shown to hold not only for two-phase composites but also for multi-phase systems.

Another interesting feature of the LLE was noted by Simpkin [3]. He found that under the condition of small Clausius-Mossotti factors,

$$\left| \frac{\epsilon_1 - \epsilon_{eff}}{\epsilon_1 + 2\epsilon_{eff}} \right| \ll 1 \tag{12}$$

and

$$\left| \frac{\epsilon_2 - \epsilon_{eff}}{\epsilon_2 + 2\epsilon_{eff}} \right| \ll 1, \tag{13}$$

the symmetric 3D Bruggeman equation follows from Equation (2). It is obvious that the conditions (12) and (13) are satisfied under a low contrast assumption, i.e., when $0.5 \ll | \epsilon_2/\epsilon_1 | \ll 2$.

Of particular interest is the case of $k = 1/3$, which corresponds to $d = 3$ and yields the LLL equation,

$$\epsilon_{eff}^{1/3} = f_1 \epsilon_1^{1/3} + f_2 \epsilon_2^{1/3}. \tag{14}$$

This equation was considered in detail by Dube [41] and Banhegui [42]. After analysing experimental data on the effective permittivity of dielectric powders at radio- and microwave frequencies, Dube concluded that Equation (14) is accurate (within 3%) up to the dielectric constant about 13, provided that the particle size exceeds 50 μm. At the same time, a comparison of experimental and calculated results for the loss factor shows much larger discrepancy, within 10–20%.

Banhegyi reviewed experimental data on the permittivity of near-spherical dielectric particles dispersed in various liquids for a wide range of filling fractions and pointed out that the LLL equation provides the best fit to experiments (within 1%) compared with several other EMA, except in the case of mineral particles in water. The latter case, however, is characterized by a relatively high dielectric contrast ($\epsilon_1/\epsilon_2 \approx 13.4$), whereas the validity

of the LLL equation is presumably limited to the regime $\mid \epsilon_1 - \epsilon_2 \mid \ll \epsilon_{eff}$, which requires a low (close-to-unity) value of ϵ_1/ϵ_2. Naturally, none of the above mixtures possesses phase-inversion symmetry. Overall, the author concluded that Equation (14) is not applicable to mixtures of nonspherical particles or to systems with high dielectric contrast, especially metal-dielectric composites.

The inconsistency of the LLL equation at high contrast h becomes evident when considering the simplest deterministic geometry possessing phase-inversion symmetry, such as a 3D regular checkerboard. In terms of conductivity, Equation (14) yields $\sigma_{eff}/\sigma_1 \to \frac{1}{8}\sigma_2/\sigma_1$ as $\sigma_2 \to \infty$, whereas the exact asymptotic result is known to be $\sigma_{eff}/\sigma_1 \to 2\sqrt{\sigma_2/\sigma_1}$ [43].

Several of recent studies also demonstrate a good predictive capability of the LLL equation, in particular, for such composite systems as iron-based powders [44], fly ash [45], and mixed magnetite-maghemite particle composites [46].

5. Archie's Law

If $k < 1/3$, except for the special cases $k = -1$ and $k = 0$, Equation (10) yields non-integer values of d. In addition, if $k > 1/3$, then $d > 3$. Since such values of d appear non-physical, this issue requires closer examination.

It is well known that for a wide variety of porous rocks with an insulating matrix saturated with a saline (conducting) fluid, the effective conductivity follows so-called Archie's law [47]

$$\sigma_{eff} = \sigma_2 f_2^m, \tag{15}$$

where σ_2 and f_2 are the conductivity and volume fraction (porosity) of the conducting fluid, respectively. The empirical parameter m is usually referred to as the cementation exponent. It is easy to see that Equation (15) follows directly from Equation (1)—expressed in terms of conductivity—under the high-contrast condition $\sigma_1/\sigma_2 \ll 1$, with $m = 1/k$ [18]. Typically, values of $m = 1.5 - 2.5$ ($k = 0.4 - 0.66$) are characteristic of most porous arenaceous sediments, while values of $m = 2.5 - 5$ ($k = 0.2 - 0.4$) occur in some carbonates [47,48].

For our purposes, it is more convenient to consider not Equation (15), but its modified version, which assumes that $\sigma_1 \neq 0$, so that both phases contribute to the effective conductivity. Modified Archie's law is given by [49]

$$\sigma_{eff} = \sigma_1(1 - f_2)^p + \sigma_2 f_2^m, \tag{16}$$

where m and p are empirical constants. Imposing the obvious condition that if $\sigma_1 = \sigma_2$, then $\sigma_{eff} = \sigma_1 = \sigma_2$, one has $(1 - f_2)^p + f_2^m = 1$. This, in turn, allows Equation (16) to be rewritten as

$$\sigma_{eff}/\sigma_1 = 1 + f_2^m\left(\frac{\sigma_2}{\sigma_1} - 1\right). \tag{17}$$

Comparing this with Equations (3) and (4) yields the only solution for the SDF: $g(x) = 0$ and $C_2 = f^{m-1}$. If this case, the second sum rule, Equation (5), breaks down, resulting in a zero first moment. Thus, strictly speaking, Archie's law is hardly consistent with the spectral representation for isotropic media.

At first sight, the above inconsistency may seem surprising and contradictory. In fact, it is important to note that although Equation (15) follows from Equation (1), it is not vice versa. While the condition of topological percolation for both phases is typically satisfied for porous media obeying Archie's law, the condition of phase-inversion symmetry is generally not met.

In Equation (5), the factor d^{-1} comes from an angular average over the directions of the applied electric field [50]. If microgeometry is anisotropic, the first moment becomes tensorial (it contains a directional dependence). Furthermore, in some cases the spatial

dependence d may become ill-defined. For instance, a quasi-2D microstructure is highly nonuniform (structured) within a plane (two directions) and nearly uniform or weakly varying along the third direction; a quasi-3D microstructure (almost isotropic 3D) may be approximately uniform along two directions and slightly non-uniform along the third. Moreover, such phenomenon as 2D-3D (or 3D-2D) crossover can occur [51–54].

6. The Analysis of Uncertainties

Because the values of the phase conductivities (permittivities) σ_i (ϵ_i) and their volume fractions f_i are always known with some uncertainty, the measured effective permittivity or conductivity is inherently uncertain. Likewise, an error in the parameter k introduces uncertainty in the calculated effective quantity. The inaccuracy of the effective conductivity $\Delta\sigma_{eff}$ for the LE can be estimated as

$$\Delta\sigma_{eff} = \frac{\partial\sigma_{eff}}{\partial k}\Delta k + \frac{\partial\sigma_{eff}}{\partial f}\Delta f + \frac{\partial\sigma_{eff}}{\partial\sigma_2}\Delta\sigma_2 + \frac{\partial\sigma_{eff}}{\partial\sigma_1}\Delta\sigma_1. \tag{18}$$

Let us now evaluate the partial derivatives $I_1 = \partial\sigma_{eff}/\partial k$, $I_2 = \partial\sigma_{eff}/\partial f$ and $I_3 = \partial\sigma_{eff}/\partial\sigma_2$ (the derivative $\partial\sigma_{eff}/\partial\sigma_1$ can be determined analogously to I_3 due to symmetry). After straightforward algebra, one obtains for $k \neq 0$:

$$I_1^{(k)} = \frac{\sigma_{eff}}{k}\left[\frac{(1-f)\sigma_1^k \ln\sigma_1 + f\sigma_2^k \ln\sigma_2}{\sigma_{eff}^k} - \ln\sigma_{eff}\right], \tag{19}$$

$$I_2^{(k)} = \frac{\sigma_{eff}^{1-k}}{k}(\sigma_2^k - \sigma_1^k), \tag{20}$$

$$I_3^{(k)} = f\left(\frac{\sigma_{eff}}{\sigma_2}\right)^{1-k}. \tag{21}$$

At $k \to 0$, using l'Hôpital's rule, one has

$$I_1^{(0)} = \frac{1}{2}f(1-f)\sigma_{eff}\ln^2(\sigma_2/\sigma_1), \tag{22}$$

$$I_2^{(0)} = \sigma_{eff}\ln(\sigma_2/\sigma_1), \tag{23}$$

$$I_3^{(0)} = f\sigma_{eff}/\sigma_2. \tag{24}$$

The values of the parameter k are usually obtained by fitting to experimental data. Since f_i and σ_1 (or ϵ_i) are known only with some uncertainty, the inaccuracy of the parameter k can be estimated as

$$\Delta k = I_1^{-1}(\Delta\sigma_{eff} - I_2\Delta f - I_3\Delta\sigma_2 - I_4\Delta\sigma_1). \tag{25}$$

It is therefore useful to estimate the partial derivative I_1.

If we are interested in small Δk, large values of the partial derivative I_1 are preferable. In the limit of $\sigma_2/\sigma_1 \to 1$, both partial derivatives I_1^0 and $I_1^{(1/3)}$ are small and attain their maximum values at $f_2 = 1/2$. As seen in Figure 2, when the contrast σ_2/σ_1 increases, the peak of I_1 shifts monotonically from lower to higher values of f_2. In particular, at $\sigma_2/\sigma_1 = 100$, $I_1^{(1/3)}$ reaches its maximum value at $f_2 \simeq 0.68$, whereas $I_1^{(0)}$ reaches its maximum at $f_2 \simeq 0.83$. In all cases, the derivative I_1 is small either when the contrast h is low (i.e., close to unity) or when f_2 is close to 0 or 1. In the limit $\sigma_2/\sigma_1 \to \infty$, the partial derivative I_1 reaches its maximum under the condition $\partial I_1/\partial f_2 = 0$. One can verify that, in this limit, the maximum of $I_1^{(0)}$ occurs as $f_2 \to 1$, while the maximum of $I_1^{(1/3)}$ occurs at $f_2 = e^{-1/3} \simeq 0.717$.

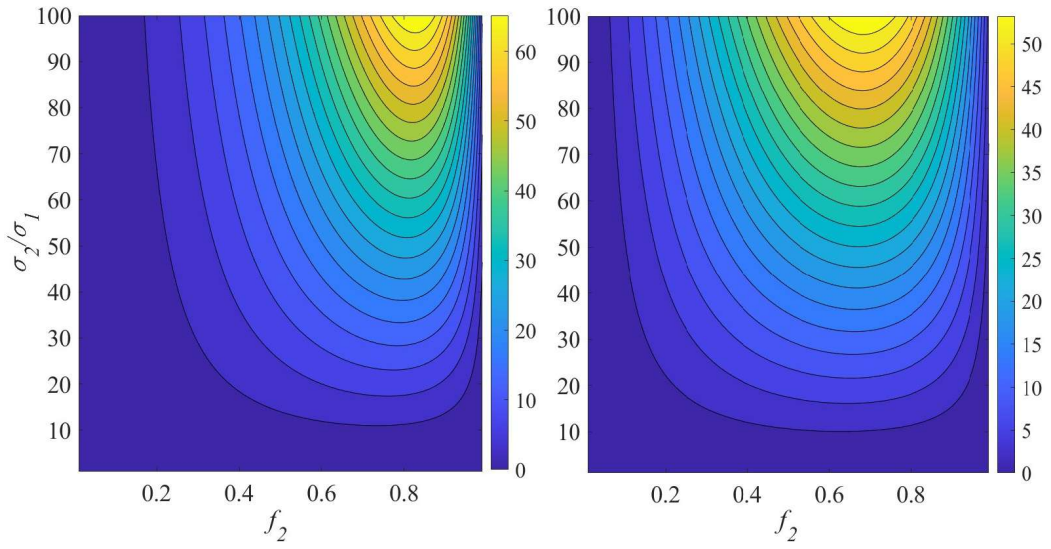


Figure 2. The partial derivatives $I_1^{(0)}$ (**left panel**) and $I_1^{(1/3)}$ (**right panel**).

7. Conclusions

In this paper, we have assessed applicability of widely used general Lichtenecker equation for isotropic composite media. The key findings of our study can be summarized as follows:

(1) The Lichtenecker equation is compatible with the spectral representation only at $k \to 0$ (logarithmic Lichtenecker equation) in 2D and $k = 1/3$ (Landau-Lifshitz-Looyenga equation) in 3D.

(2) In 3D, the Lichtenecker equation is applicable only for low contrast h, even for composites possessing phase-inversion symmetry.

(3) Although Archie's is confirmed in many experiments for porous media, this does not, by itself, validate the Lichtenecker equation.

(4) If the empirical parameter k of the Lichtenecker equation is determined by fitting to experimental data, small errors in phase volume fractions and/or their conductivities and permittivities can lead to significant inaccuracies in k, especially when f_2 is close to 0 or 1, or when the contrast parameter h is low.

In conclusion, great care must be taken when using the Lichtenecker equation, particularly for the effective permittivity or conductivity of metal-dielectric mixtures. Although it sometimes yields reasonable results, in most cases its use is not physically justified.

Author Contributions: Conceptualization, A.V.G. and V.M.S.; methodology, A.V.G.; software, A.V.G.; validation, A.V.G. and V.M.S.; formal analysis, A.V.G.; investigation, A.V.G. and V.M.S.; resources, A.V.G. and V.M.S.; data curation, A.V.G.; writing—original draft preparation, A.V.G.; writing—review and editing, A.V.G. and V.M.S.; visualization, A.V.G.; supervision, V.M.S.; project administration, V.M.S.; funding acquisition, V.M.S. All authors have read and agreed to the published version of the manuscript.

Funding: This research was funded by the Spanish Ministry of Science and Innovation, Grants No. TED2021-132074B-C32 and PID2022-139230NB-I00.

Institutional Review Board Statement: Not applicable.

Data Availability Statement: The original contributions presented in this study are included in the article. Further inquiries can be directed to the corresponding author.

Conflicts of Interest: The authors declare no conflict of interest. The funders had no role in the design of the study; in the collection, analyses, or interpretation of data; in the writing of the manuscript; or in the decision to publish the results.

References

1. Lichtenecker, K. Die Dielektrizitätskonstante natürlicher und künstlicher Mischkörper. *Phys. Z.* **1926**, *27*, 115–158.
2. Lichtenecker, K. Der elektrische Leitungswiderstand künstlicher und natürlicher Aggregate. *Phys. Z.* **1924**, *25*, 225–233.
3. Simpkin, R. Derivation of Lichtenecker's logarithmic mixture formula from Maxwell's equations. *IEEE Trans. Microw. Theory Tech.* **2010**, *58*, 545–550. [CrossRef]
4. Erle, U.; Regier, M.; Persch, C.; Schubert, H. Dielectric properties of emulsions and suspensions: Mixture equations and measurement comparisons. *J. Microw. Power Electromag. Energy* **2000**, *35*, 185–190. [CrossRef]
5. Yan, Y.; Gonzalez-Cortes, S.; Yao, B.; Slocombe, D.R.; Porch, A.; Cao, F.; Xiao, T.; Edwards, P.P. Rapid, non-invasive characterization of the dispersity of emulsions via microwaves. *Chem. Sci.* **2018**, *9*, 6975–6980. [CrossRef]
6. Robinson, D.A.; Jones, S.B.; Wraith, J.M.; Or, D.; Friedman, S.P. A review of advances in dielectric and electrical conductivity measurement in soils using time domain feflectometry. *Vadose Zone J.* **2003**, *2*, 444–475. [CrossRef]
7. Su, C.; Wu, C.C.; Yang, C. Developing the dielectric mechanisms of polyetherimide/multiwalled carbon nanotube/$(Ba_{0.8}Sr_{0.2})(Ti_{0.9}Zr_{0.1})O_3$ composites. *Nanoscale Res. Lett.* **2012**, *7*, 132. [CrossRef] [PubMed]
8. Headland, D.; Thurgood, P.; Stavrevski, D.; Withayachumnankul, W.; Abbott, D.; Bhaskaran, M.; Sriram, S. Doped polymer for low-loss dielectric material in the terahertz range. *Opt. Mater. Express* **2015**, *5*, 1373–1380. [CrossRef]
9. Pérez-Campos, R.; Monzó-Cabrera, J.; Fayos-Fernández, J.; Díaz-Morcillo, A.; Martínez-González, A.; Lozano-Guerrero, A.; Pedreño-Molina, J.; García-Gambín, J. Dielectric characterization of fabric aggregates around the 2.45 GHz ISM band under various humidity, density, and temperature conditions. *Materials* **2023**, *16*, 4428. [CrossRef] [PubMed]
10. Kiley, E.M.; Yakovlev, V.V.; Ishizaki, K.; Vaucher, S. Applicability study of classical and contemporary models for effective complex permittivity of metal powders. *J. Microw. Power Electromag. Energy* **2012**, *46*, 26–38. [CrossRef]
11. Akhtar, M.J.; Tiwari, N.K.; Devi, J.; Mahmoud, M.; Link, G.; Thumm, M. Determination of effective constitutive properties of metal powders at 2.45 GHz for microwave processing applications. *Frequenz* **2014**, *68*, 69–81. [CrossRef]
12. Xiao, X.; Ihamouten, A.; Villain, G.; Dérobert, X. Use of electromagnetic two-layer wave-guided propagation in the GPR frequency range to characterize water transfer in concrete. *NDT E Intern.* **2017**, *86*, 164–174. [CrossRef]
13. Hickson, D.; Boivin, A.; Daly, M.G.; Ghent, R.; Nolan, M.C.; Tait, K.; Cunje, A.; Tsai, C.A. Near surface bulk density estimates of NEAs from radar observations and permittivity measurements of powdered geologic material. *Icarus* **2018**, *306*, 16–24. [CrossRef]
14. Balčiūnas, S.; Ivanov, M.; Banys, J.; Ueno, S.; Wada, S. In search of an artificial morphotropic phase boundary: Lead-free barium titanate based composites. *Lith. J. Phys.* **2020**, *60*, 225–234. [CrossRef]
15. Boughriet, A.; Allahdin, O.; Poumaye, N.; Tricot, G.; Revel, B.; Lesven, L.; Wartel, M. Micro-analytical study of a zeolites/geo-polymers/quartz composite, dielectric behaviour and contribution to Brønsted sites affinity. *Ceramics* **2022**, *5*, 908–927. [CrossRef]
16. Anandakrishnan, S.S.; Nelo, M.; Tabeshfar, M.; Kraft, V.; Khansur, N.H.; Peräntie, J.; Bai, Y. Influence of the permittivity between fillers and binders on the properties of upside-down composites for recycling purposes. *Mater. Adv.* **2025**, *6*, 6694–6710. [CrossRef]
17. de Lima, O.A.L.; Clennell, M.B.; Nery, G.G.; Niwas, S. A volumetric approach for the resistivity response of freshwater shaly sandstones. *Geophysics* **2005**, *70*, F1–F10. [CrossRef]
18. Glover, P. A generalized Archie's law for n phases. *Geophysics* **2010**, *75*, E247–E265. [CrossRef]
19. Antepara, I.; Fiala, L.; Pavlík, Z.; Černý, R. Moisture dependent thermal properties of hydrophilic mineral wool: Application of the effective media theory. *Mater. Sci. (Medžiagotyra)* **2015**, *21*, 449–454. [CrossRef]
20. Fuchs, S.; Schütz, F.; Förster, H.J.; Förster, A. Evaluation of common mixing models for calculating bulk thermal conductivity of sedimentary rocks: Correction charts and new conversion equations. *Geothermics* **2013**, *47*, 40–52. [CrossRef]
21. Parke, L.; Hooper, I.R.; Hicken, R.J.; Dancer, C.E.J.; Grant, P.S.; Youngs, I.J.; Sambles, J.R.; Hibbins, A.P. Heavily loaded ferrite-polymer composites to produce high refractive index materials at centimetre wavelengths. *APL Mater.* **2013**, *1*, 042108. [CrossRef]
22. Wang, Y.; Edwards, E.; Hooper, I.; Clow, N.; Grant, P.S. Scalable polymer-based ferrite composites with matching permeability and permittivity for high-frequency applications. *Appl. Phys. A* **2015**, *120*, 609–614. [CrossRef]
23. Kočí, V.; Maděra, J.; Krejčí, T.; Kruis, J.; Černý, R. Efficient techniques for solution of complex computational tasks in building physics. *Adv. Civil Eng.* **2019**, *2019*, 3529360. [CrossRef]
24. Guo, R.; Roscow, J.; Bowen, C.; Luo, H.; Huang, Y.; Ma, Y.; Zhou, K.; Zhang, D. Significantly enhanced permittivity and energy density in dielectric composites with aligned BaTiO3 lamellar structures. *J. Mater. Chem. A* **2020**, *8*, 3135–3144. [CrossRef]
25. Schulgasser, K. On a phase interchange relationship for composite materials. *J. Math. Phys.* **1976**, *17*, 378–381. [CrossRef]
26. Stroud, D.; Milton, G.W.; De, B.R. Analytical model for the dielectric response of brine-saturated rocks. *Phys. Rev. B* **1986**, *34*, 5145–5153. [CrossRef]

27. Ghosh, K.; Fuchs, R. Spectral theory for two-component porous media. *Phys. Rev. B* **1988**, *38*, 5222–5236. [CrossRef] [PubMed]
28. Ghosh, K.; Fuchs, R. Critical behavior in the dielectric properties of random self-similar composites. *Phys. Rev. B* **1991**, *44*, 7330–7333. [CrossRef]
29. Tuncer, E. Geometrical description in binary composites and spectral density representation. *Materials* **2010**, *3*, 585–613. [CrossRef]
30. Fuchs, R.; Ghosh, K. Optical and dielectric properties of self-similar structures. *Phys. A* **1994**, *207*, 185–196. [CrossRef]
31. Goncharenko, A.V. Spectral density function approach to homogenization of binary mixtures. *Chem. Phys. Lett.* **2004**, *400*, 462–468. [CrossRef]
32. Tuncer, E.; Bowler, N.; Youngs, I.J. Application of the spectral density function method to a composite system. *Phys. B* **2006**, *373*, 306–312. [CrossRef]
33. Dmitruk, N.L.; Goncharenko, A.V.; Venger, E.F. *Optics of Small Particles and Composite Media*; Naukova Dumka: Kyiv, Ukraine, 2009.
34. Goncharenko, A.V.; Lozovski, V.Z.; Venger, E.F. Lichtenecker's equation: Applicability and limitations. *Opt. Commun.* **2000**, *174*, 19–32. [CrossRef]
35. Looyenga, H. Dielectric constants of heterogeneous mixtures. *Physica* **1965**, *31*, 401–406. [CrossRef]
36. Landau, L.D.; Lifshitz, E.M. *Electrodynamics of Continuous Media*; Pergamon Press: Oxford, UK; New York, NY, USA; Beijing, China; Frankfurt, Germany, 1984.
37. Keller, J.B. The theorem on the conductivity of a composite medium. *J. Mathem. Phys.* **1964**, *5*, 548–549. [CrossRef]
38. Dykhne, A.M. Conductivity of a two-dimensional two-phase system. *Sov. Phys. JETP* **1971**, *32*, 63–65; Translation of *Zh. Eksp. Teor. Fiz.* **1970**, *59*, 110–115.
39. Machavariani, V.S.; Voronel, A. Estimation of the intrinsic heterogeneity of ionic glass-forming melts. *Phys. Rev. E* **2000**, *61*, 2121–2124. [CrossRef] [PubMed]
40. Machavariani, V.S. Universality in effective conductivity of regular 2D and 3D composites. *J. Phys. Condens. Matter* **2001**, *13*, 6797–6812. [CrossRef]
41. Dube, D. Study of Landau-Lifshitz-Looyenga's formula for dielectric correlation between powder and bulk. *J. Phys. D Appl. Phys.* **1970**, *3*, 1648–1652. [CrossRef]
42. Bánhegyi, G. Comparison of electrical mixture rules for composites. *Colloid Polym. Sci.* **1986**, *264*, 1030–1050. [CrossRef]
43. Soderberg, M.; Grimvall, G. Current distributions for a two-phase material with chequer-board geometry. *J. Phys. Solid State Phys.* **1983**, *16*, 1085. [CrossRef]
44. Yang, R.B.; Hsu, S.D.; Lin, C.K. Frequency-dependent complex permittivity and permeability of iron-based powders in 2–18 GHz. *J. Appl. Phys.* **2009**, *105*, 07A527. [CrossRef]
45. Sreenivas, V.N.; Karthik, D.; Kumar, V.A. Determination of complex permittivity of fly ash for potential electronic applications. *Appl. Mech. Mater.* **2012**, *110–116*, 4292–4296. [CrossRef]
46. Sainz-Menchón, M.; González de Arrieta, I.; Echániz, T.; Nader, K.; Insausti, M.; Canizarès, A.; Rozenbaum, O.; López, G. Quantifying lattice vibrational modes and optical conductivity in mixed magnetite–maghemite nanoparticles. *Phys. Chem. Chem. Phys.* **2025**, *27*, 8498–8509. [CrossRef]
47. Cai, J.; Wei, W.; Hu, X.; Wood, D.A. Electrical conductivity models in saturated porous media: A review. *Earth Sci. Rev.* **2017**, *171*, 419–433. [CrossRef]
48. Glover, P. What is the cementation exponent? A new interpretation. *Lead. Edge* **2009**, *28*, 82–85. [CrossRef]
49. Glover, P.W.; Hole, M.J.; Pous, J. A modified Archie's law for two conducting phases. *Earth Planet. Sci. Lett.* **2000**, *180*, 369–383. [CrossRef]
50. Kantor, Y.; Bergman, D.J. Improved rigorous bounds on the effective elastic moduli of a composite material. *J. Mech. Phys. Solids* **1984**, *32*, 41–62. [CrossRef]
51. Gelb, L.D.; Gubbins, K.E.; Radhakrishnan, R.; Sliwinska-Bartkowiak, M. Phase separation in confined systems. *Rep. Prog. Phys.* **1999**, *62*, 1573. [CrossRef]
52. Dvoynenko, M.M.; Goncharenko, A.V.; Romaniuk, V.R.; Venger, E.F. Effects of dimension on optical transmittance of semicontinuous gold films. *Phys. B* **2001**, *299*, 88–93. [CrossRef]
53. Mokhtari, M.; Zekri, L.; Kaiss, A.; Zekri, N. Effect of film thickness on the width of percolation threshold in metal-dielectric composites. *Condens. Matter Phys.* **2016**, *19*, 43001. [CrossRef]
54. Chalyi, A.V. Effective fractal dimension at 2d-3d crossover. *Fract. Fract.* **2022**, *6*, 739. [CrossRef]

Disclaimer/Publisher's Note: The statements, opinions and data contained in all publications are solely those of the individual author(s) and contributor(s) and not of MDPI and/or the editor(s). MDPI and/or the editor(s) disclaim responsibility for any injury to people or property resulting from any ideas, methods, instructions or products referred to in the content.